Appearance of a conductive carbonaceous coating in a CO_2 Dielectric Barrier Discharge and its influence on the electrical properties and the conversion efficiency.

Igor Belov[1,2], Sabine Paulussen[1] and Annemie Bogaerts[2]

[1] VITO, Sustainable Materials Management, Mol, Belgium
[2] University of Antwerp, PLASMANT, Antwerp, Belgium

E-mail: igor.belov@vito.be

Abstract

This work examines the properties of a dielectric barrier discharge (DBD) reactor, built for CO_2 decomposition, by means of electrical characterization, optical emission spectroscopy and gas chromatography. The discharge, formed in an electronegative gas (such as CO_2, but also O_2), exhibits clearly different electrical characteristics, depending on the surface conductivity of the reactor walls. An asymmetric current waveform is observed in the metal-dielectric (MD) configuration, with sparse high-current pulses in the positive half-cycle (HC) and a more uniform regime in the negative HC. This indicates that the discharge is operating in two alternating regimes with rather different properties. At high CO_2 conversion, a conductive coating is deposited on the dielectric. This so-called coated MD configuration yields a symmetric current waveform, with current peaks in both the positive and negative HCs. In a double-dielectric (DD) configuration, the current waveform is also symmetric, but without current peaks in both the positive and negative HC. Finally, the DD configuration with conductive coating on the inner surface of the outer dielectric, i.e., so-called coated DD, yields again an asymmetric current waveform, with current peaks in the negative HC. These different electrical characteristics are related to the presence of the conductive coating on the dielectric wall of the reactor and can be explained by an increase of the local barrier capacitance available for charge transfer. The different discharge regimes affect the CO_2 conversion, more specifically, the CO_2 conversion is lowest in the clean DD configuration. It is somewhat higher in the coated DD configuration, and still higher in the MD configuration. The clean and coated MD configuration, however, gave similar CO_2 conversion. These results indicate that the conductivity of the dielectric reactor walls can highly promote the development of the high-amplitude discharge current pulses and subsequently the CO_2 conversion.

Subject classification numbers
81.20Ka, 52.80Hc

1. Introduction

Carbon dioxide plays a complex role in the modern world. On the one hand, it is a ubiquitous by-product of chemical processing and fuel combustion and thus a major contributor to the greenhouse effect. On the other hand, CO_2 has a very good potential to be a negative value raw material for the chemical industry and, possibly, a feedstock for alternative fuels. The conversion of pure CO_2 flow into base chemicals is one of the possible pathways for carbon-containing waste valorization. A lot of new approaches to develop a robust and energy-efficient technology for CO_2 decomposition by means of non-thermal plasma, either pure or mixed with a H-source, like CH_4 or H_2O, is being investigated [1].

Dielectric barrier discharge (DBD) systems exploit the properties of non-thermal plasmas and represent one of the possible solutions for CO_2 decomposition technology. A coaxial DBD reactor geometry, in which one or both electrodes are covered with dielectric material, is commonly used for this process [2,3] while a parallel plate design is utilized to apply optical diagnostics to the system [4,5]. The most common approaches towards achieving higher values of CO_2 conversion efficiency include variation of reactor geometry [6], materials [7-9], the introduction of packing materials [10,11] or an admixture gas [12-14]. All of the aforementioned work relies on electrical characterization as one of the diagnostic methods in order to evaluate the power input and to monitor the discharge process. For instance, in the works by Li *et al.* [7,8] the implementation of high-permittivity dielectric materials resulted in establishing distinct high-current pulses and consequently a higher power discharge.

In this paper, we investigate in first instance the asymmetric current waveforms of a CO_2 discharge, composed of high-amplitude sparse peaks in the positive half-cycle (HC) and limited discharge current in the negative one. An asymmetry of the current waveform of the CO_2 discharge was indeed also observed in literature for a system with a metal electrode and an electrode covered with a dielectric material (further denoted as MD configuration) [2,7] and suggests the dissimilarity of microdischarge activity in the positive and negative HC. This phenomenon could be expected, given the asymmetric nature of a coaxial DBD reactor in a MD configuration [15,16] and the principles of microdischarge formation [17-19]. Nevertheless, the asymmetric properties of the discharge activity are mostly reported for surface barrier discharge set-ups [20-24] and asymmetric current waveforms consisting of uniform glow-like and strong filamentary phases are typically observed for these systems [25-27]. Depending on the polarity of the applied voltage, the half-cycles are denoted as M+D- when the metal electrode is positive and M-D+ in the other case. Folkstein *et al.* studied the asymmetry of the microdischarge properties in N_2-O_2 mixtures and found that M-D+ microdischarges are less intense, but more frequent than M+D- ones [28]. Hoder *et al.* observed differences in the microdischarge development and propagation in various single filament DBD reactor configurations by means of cross-correlation spectroscopy [19]. Osawa and Yoshika demonstrated an asymmetrical current waveform using a 50 Hz DBD system operating with two different dielectric materials [29].

During the CO_2 splitting experiments reported in this work, a conductive coating was found on the reactor walls. It was considered to be a carbon film, resulting from the CO_2 decomposition process. Interestingly, coke deposition during pure CO_2 processing in a DBD reactor is typically not observed by other authors [3,4,30]. Zheng *et al.* found solid carbonates only when using CO as a feed gas instead of CO_2 [12]. On the other hand, Li *et al.* also observed carbon deposition, and associated this to the high-current discharge peaks, resulting from the use of a high-permittivity dielectric [8]. Tomai *et al.* utilized a DBD reactor under super-critical conditions to achieve carbon deposition from CO_2 feedthrough [31,32].

An interesting implication of conductive carbon deposition on the electrodes is the modification of the electrical signal of the CO_2 discharge. A shift from an asymmetric current waveform to a symmetric one was observed and attributed to the appearance of a conductive film on the dielectric surface. To the best of our knowledge, this effect was not described before, although the influence of the dielectric material conductivity or of conductive coatings on the dielectric material was investigated for various gas mixtures [9,33-35]. Both Kim *et al* and Choi *et al* correlated the improvement of N_2 discharge uniformity to the conductivity of the dielectric surface

[33,34]. Guoqing *et al.* observed a decrease in the number of filaments and in the discharge power for the case of highly conductive dielectric surfaces in a N_2-Ar mixture [35]. Wang *et al*. reported a higher discharge current and efficiency of CO_2 conversion in the MD reactor by means of custom-made high-permittivity dielectrics with a higher concentration of glass, i.e. a lower surface resistivity [9]. In this way the effect of the high-permittivity dielectric conductivity on the CO_2 discharge in the MD configuration was explored. However, it is not clear yet whether it is possible to modulate the CO_2 discharge current and CO_2 conversion by means of enhancing the conductivity of conventional dielectric material surfaces (e.g. borosilicate glass, alumina).

To address this problem, we also explored a double dielectric (DD) configuration of a DBD reactor, and we compared it to the MD one, by applying a conductive coating on one of the dielectric layers of the DD reactor. Falkstein *et al.* examined the different operation of the DD configuration in dry and wet air, and associated the rise of microdischarge amplitude with a water film appearing on the electrodes [28]. Brehmer *et al.* utilized the quartz DD reactor for CO_2 decomposition and observed a symmetric waveform with limited discharge current amplitude of about 35 mA, and no carbon deposition was found during the process [5]. Tu *et al.* used the DD configuration for dry reforming of methane in a mixture of CH_4 and CO_2 and observed coke deposition, although the effect of the coating on the electrical properties or conversion was not discussed [36]. Clearly, there is a lack of understanding in how the reactor walls conductivity can influence the discharge regime and thus the CO_2 conversion. Moreover, such a study is also crucial from the industrial point of view, as the contamination of the electrodes is inevitable in a large scale operation. In our study, the introduction of a conductive coating on one of the dielectric walls of the DD configuration significantly enhances the discharge current in one of the HCs and subsequently the CO_2 conversion. To the best of our knowledge, this effect was not yet reported before.

In general, it is clear that the surface conductivity of the dielectric walls can greatly influence the electrical current profiles, and thus also the CO_2 conversion, but a systematic study of these effects has not yet been performed. This is exactly the aim of the present work.

2. Experimental part

2.1. Reactor set-up

The experimental setup is schematically shown in figure 1. In case of the MD configuration (figure 1, a), a cylindrical discharge gap of 0.5 mm is obtained between a grounded stainless steel central electrode (outer diameter 25 mm) and a dielectric tube (26 mm inner diameter, 29 mm outer diameter) made of borosilicate glass or alumina. It was demonstrated by Aerts *et al.* [6] that using a smaller gap allows the rise of the reactor capacitance and a decrease of the onset voltage due to enhanced electric field intensity, thus it is beneficial for the system performance. A stainless steel mesh is wrapped at the outside of the dielectric tube, acting as an outer electrode and at the same time defining the length of the plasma (215 mm). The outer electrode arrangement is cooled with deionized water with a controlled conductivity of less than 0.5 μS·m. In this way, local overheating of the reactor and parasitic discharges on the sharp edges of the mesh are prevented. The central electrode is cooled with drinking water of standard quality.

The DD configuration (figure 1, b) is similar to the MD reactor with respect to the arrangement of the electrodes. The central electrode is in this case a quartz tube, filled with technical quality water, i.e. conductive water. A grounded stainless steel rod is introduced into the liquid for sustaining electrical contact. Water is circulated for cooling of the quartz tube.

The outer electrode is in both cases connected to a power supply with a maximum peak-to-peak voltage of 40 kV and a variable frequency between 2 and 90 kHz (AFS G10S-V generator, AFS GT-10...80 transformers). The applied voltage is measured by a high voltage probe (Tektronics P6015A) and the total current is obtained by a Rogowski-type current meter (Pearson Model 4100, 35 MHz). Due to the design of the reactor it was not possible to introduce an external measuring capacitor in the electrical circuit of the reactor. This diagnostic tool is implemented only in the DD configuration of the reactor, where a 5.5 nF capacitance is installed in series with the grounded electrode to obtain the transferred charge – voltage (Q-U) characteristics.

The process is monitored by a 25 MHz PicoScope 2205 digital oscilloscope, while the electrical signals are recorded by a 2.5 GS/s 500MHz Tektronics TDS 3052 (S/s = number of samples per second). In our system, the energy input in the discharge is controlled by setting the power of the generator and calculating the corresponding value (equation 1):

$$P_{Input} = \frac{1}{T}\int_0^T I(t)U(t)dt \quad (1)$$

where T is the period of the AC, and $I(t)$ and $U(t)$ are the measured current and applied voltage signals, respectively. Previous calorimetric studies of the system confirmed the accuracy of this method.

Table 1 summarizes the properties of the MD and DD reactor configurations.

Table 1. Summary of the reactor properties in both the MD and DD configuration

	Reactor type	
Property	MD configuration	DD configuration
Gap, mm	0.5	0.5
Length of discharge zone, mm	215	215
Outer dielectric	Alumina or borosilicate glass	Alumina or borosilicate glass
Inner dielectric	-	Quartz
Discharge cell capacitance, pF	330 or 250 (for alumina or glass dielectric, resp.)	175 or 150 (for alumina or glass dielectric, resp.)
External capacitance, pF	-	5500

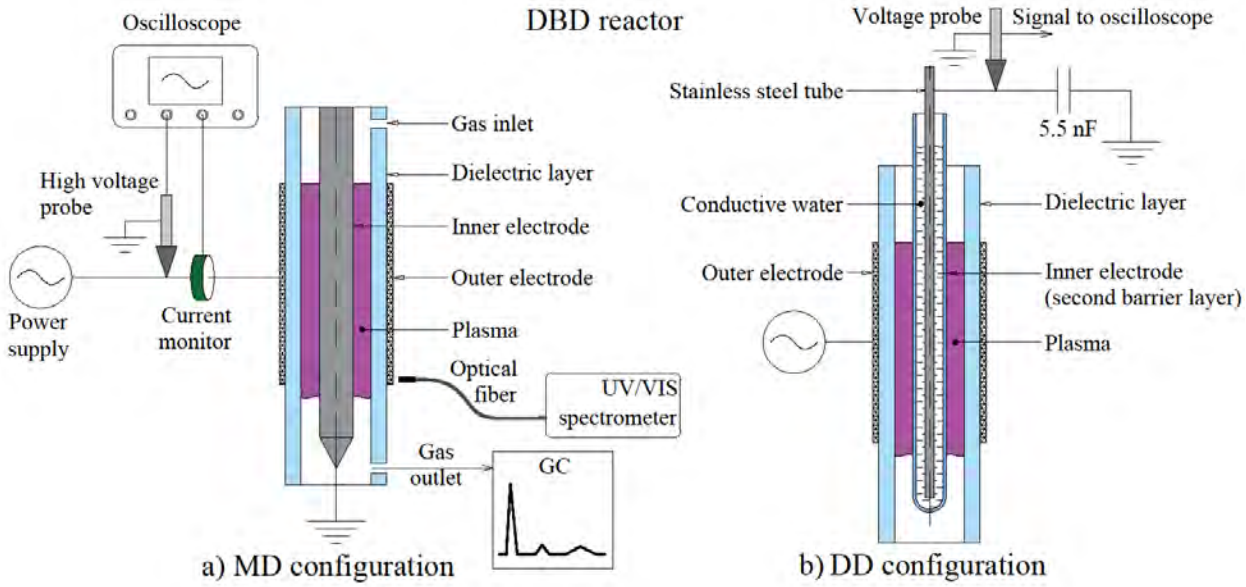

Figure 1. Experimental setup of the coaxial dielectric barrier discharge reactor: *a)* metal-dielectric (MD) and *b)* double-dielectric (DD) configurations (the same analysis systems are applied and not shown here).

2.2. Process conditions

In case of a 0.5 mm discharge gap and 215 mm steel mesh length, the total volume of the reactor equals 8.6 mL. The gas flow rate is varied from 0.05 to 0.6 SLM of CO_2, yielding a residence time between 10.3 and 0.86 seconds. Similar flow rates are also applied for N_2 and O_2 feedthrough (see below). CO_2 gas of industrial quality (99.5% purity, Air Products) is used in this set of experiments. The gaseous products of the reaction are analysed by gas chromatography (Trace-GC, Interscience), equipped with a thermal conductivity detector (TCD). The conversion of CO_2 is calculated by comparing the peak area of CO_2 in the TCD signal before and after plasma exposure (equation 2) and the carbon balance is estimated according to equation 3:

$$CO_2\ \text{Conversion}(\%) = [1 - \frac{molesCO_{2,\ Plasma\ \ ON}}{molesCO_{2,\ Plasma\ \ OFF}}] \times 100\% \quad (2)$$

$$\text{Carbon balance}(\%) = \frac{molesCO_{2,\ Plasma\ \ ON} + molesCO_{Plasma\ \ ON}}{molesCO_{2,\ Plasma\ \ OFF}} \times 100\% \quad (3)$$

The specific energy input (SEI) is used to compare the conversion efficiencies of the various set-ups (equation 4) [37]:

$$\text{SEI (eV/molec.)} = \frac{P_{Input}(W) \cdot 60(s/\min)}{Flow\,rate(ml/\min) \cdot 3.92(eV \cdot ml/J \cdot molec)} \quad (4)$$

A UV/VIS (180-750 nm) survey fiber spectrometer (Avantes, AvaSpec 2048) with 2.3 nm FWHM resolution is used for monitoring the process in both reactors, collecting light through a 6 mm collimating lens. The lens was pointed on the gas gap through the optical window (90% transmittance in the 320-600 nm range) installed downstream the reactor parallel to the electrode axis. The same electrical analysis and gas chromatography systems are applied for the experiments in the MD and DD reactors.

3. Results and discussion

3.1. Electrical characteristics for the MD configuration

Figure 2 shows the applied voltage and measured current waveforms of the MD DBD configuration for CO_2, as well as for O_2 and N_2. Besides the electronegative gases, like CO_2 and O_2, we also investigated N_2, to compare the electrical signals of the discharges. As the critical electric field for N_2 breakdown is lower than that of CO_2 or O_2, a rather different discharge behaviour might be expected . It is known that the total current is a superposition of a quasi-sinusoidal displacement one and numerous discharge pulses. The former corresponds to the capacitive nature of the DBD system and does not depend on the gas composition. Meanwhile, the latter gives evidence for the filamentary character of the discharge, consisting of randomly distributed individual filaments, although the amplitude of these current pulses for CO_2 and O_2 is clearly higher than for N_2. Moreover, the current waveform of the CO_2 and O_2 discharge appears to be asymmetric, i.e. the discharge current in the positive HC has a different structure than in the negative one.

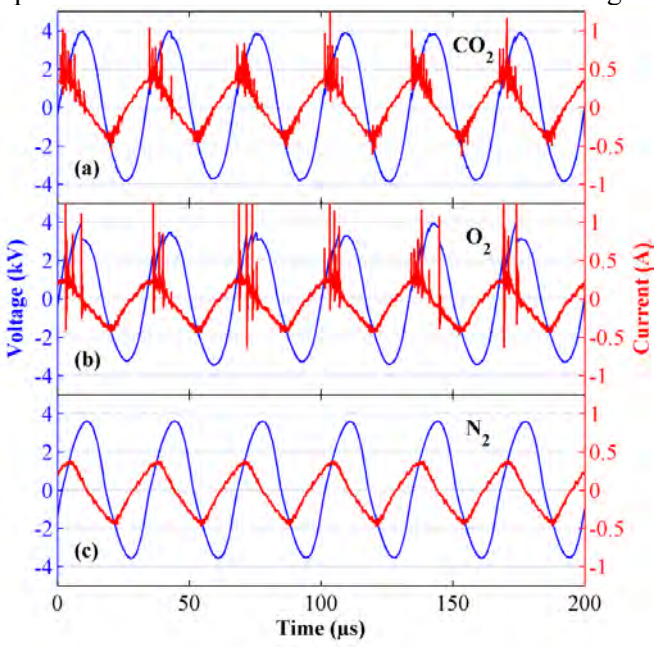

Figure 2. Electrical signal of the DBD reactor in the MD configuration: *(a)* CO_2; *(b)* O_2; *(c)* N_2. (discharge power: 180W; feed flow rate: 0.2 SLM; frequency: 30 kHz for all three cases; dielectric material: alumina).

One period of applied voltage, in case of the CO_2 discharge, is shown in figure 3, after subtraction of the displacement current from the total current. The discharge current in the positive HC is composed of relatively high sparse peaks (with values up to 1-2 A) and the applied voltage waveform is correspondingly distorted by sharp voltage drops up to 1 kV, while a more uniform discharge appears in the negative HC. Interestingly, this remarkable asymmetric behaviour was not observed for the N_2 discharge at the same conditions (fig. 2, c) or other tested gases (Ar, CH_4). This feature of the CO_2 discharge is observed for the whole range of discharge gaps examined in our system, ranging from 0.5 to 2 mm, i.e. a central electrode outer diameter between 25 and 22 mm.

Besides the bandwidth of the oscilloscope, the sampling rate (represented in number of samples per second) is the parameter that might influence the precision of measurements. Depending on the frequency of the applied voltage the oscillograms were recorded with a sampling rate from 10 MS/s to 50 MS/s (million samples per second). Up to the tested 2.5 GS/s, the asymmetric structure described above was preserved.

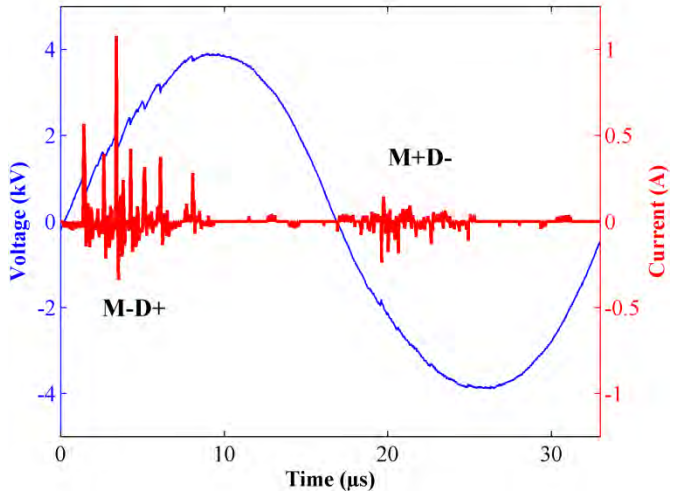

Figure 3. Electrical signal in one period of applied voltage for the CO_2 discharge (discharge power: 180W; feed flow rate: 0.2 SLM; frequency: 30 kHz; dielectric material: alumina).

The comparison of the pulses for positive and negative HC is presented in figure 4. The rise time of the current peaks is about 10 ns and is similar for both HCs. This value is close to usable rise time. The ringing of the current signal is observed after the current pulse propagation. This effect is known to be a drawback of Rogowski coil current meters [25] responsible for the 5% observed uncertainty during the power measurements.

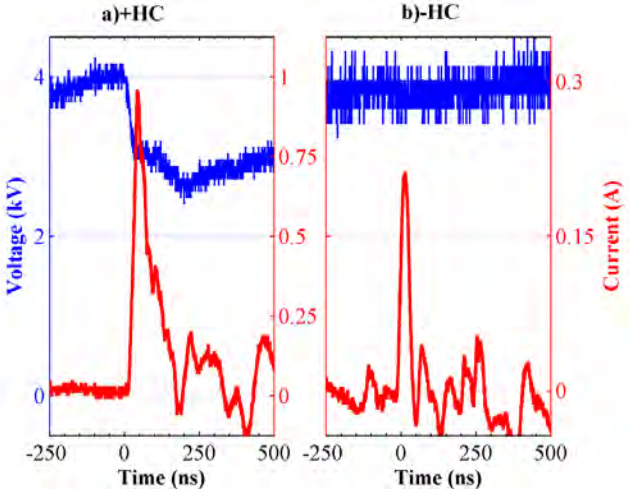

Figure 4. Measured current and voltage signal for positive (a) and negative (b) HC (180W-0.2SLM CO_2-30 kHz).

An asymmetric current waveform was also observed by Guaitella *et al.* [38] in a similar metal-dielectric DBD (6 mm gap) system operating in air at 50 Hz excitation frequency. Remarkably, the high-current structure was observed in the M+D- polarity ("M+Q-" notation used in the paper), which is opposite to our observations. A structure similar to our case of the CO_2 discharge current was observed by Li *et al.* in the MD configuration, although the reported waveforms were not so irregular in the positive and negative half-cycles, possibly because of the high-permittivity dielectric being used [7,8]. The distortion of the voltage signal might be related to the reaction of the power supply to the high current pulses. A somewhat similar behaviour in terms of current discharge asymmetry and amplitude can be seen on the oscillograms presented by Mei *et al.* for a system with a wider discharge gap of 3 mm [10]. In the work by Aerts *et al.* [6], modifications in the waveform due to a rise in discharge gap or energy input variations were presented. No clear asymmetry was observed in this study, and the discharge current amplitude was somewhat lower than in our system. Ramakers *et al.* explored the discharge properties in mixtures of CO_2 with Ar and He [14]. Notably different waveforms were presented both for the case of discharges of pure CO_2 and CO_2 diluted with Ar. As will be shown below, the asymmetry of the current waveform is highly dependent on the surface quality of the dielectric material. Contaminated or aged dielectrics can yield a symmetric waveform for a discharge in CO_2. Another point is that the mesh electrode exposed to the atmosphere can induce a parasitic discharge, which will create additional noise in the current measurements. Finally, the discharge conditions (discharge gap, gas flow rate, applied frequency) used by Aerts *et al.* [6] and Ramakers *et al.* [14] were somewhat different, so it is dangerous to draw conclusions about the different current waveforms.

From the presented waveforms (figures 2 and 3), it can be concluded that the discharge current and consequently also the charge transfer in case of the electronegative gases (CO_2 and O_2) are significantly more established in the positive half-cycle of the applied voltage, when the grounded electrode has a negative polarity (M-D+ configuration), compared to the negative half-cycle (M+D-). This behavior is similar to the asymmetric properties of surface barrier discharges [20-27] but is in distinct contradiction with the studies of microdischarge formation in a N_2-O_2 atmosphere [28,39], where more intense and irregular microdischarges were reported for the M+D- configuration. Moreover, prominent decrease of the microdischarge amplitude was correlated with addition of oxygen. However, considering the electronegativity of CO_2 and O_2 and the lower ionization potential of these gases compared to N_2 (i.e., 13.8 and 12.1 eV, vs. 15.6 eV), one might expect sparse and high intensity filaments for the CO_2 and O_2 discharges. Audier *et al.* studied the morphology of surface barrier discharges in mixtures of N_2-O_2 [40]. It was shown that the addition of the electronegative oxygen gas results in fewer, stronger and brighter filaments. Notably, in pure O_2 the current pulses were the strongest, as more filaments were ignited at the same locations, utilizing the strong channels of the extinguished filaments. This is also in correlation with our results, where no strong current peaks were observed in the electropositive N_2 discharge, in contrast to the electronegative CO_2 and O_2 discharges. It might appear that the high current pulses are limited by the capacitance available for a single filament. A somewhat similar behavior was shown experimentally (for the CO_2 discharge) by Li *et al.* [7,8] and theoretically by Akishev *et al* [41,42]. Accordingly, the MD discharge asymmetry might be explained by this hypothesis: the capacity of the electron supply (i.e. charge transferred after streamer breakdown) of the M-D+ polarity is significantly larger than in the case of the M+D- one. This allows the flow of the high-current pulses of the CO_2 or O_2 discharges in the M-D+ configuration, while the discharge current peaks are limited in the M-D+ polarity. The current waveforms present an integrated picture of a bulk discharge, i.e. we cannot deconvolute the information out of it for a single microdischarge. Nevertheless, we can conclude that the microdischarge activity processes are different in the M+D- and the M-D+ configurations.

3.2. Effect of a conductive film on the discharge properties

During the experiments on CO_2 decomposition, it was noted that a black-coloured coating was deposited both on the central metal electrode and on the inner surface of the dielectric tube. The formation of the film was observed for both of the tested dielectric materials, i.e. alumina and borosilicate glass. The coating showed a good adhesion to the metal electrode; sand paper had to be

used to clean the surface afterwards. For the borosilicate glass, the adhesion was not so strong and the coating could be removed with a tissue. In the case of the alumina dielectric, a not well-adhered layer was found on top of a rather sticky coating, which could not be easily removed. The achieved coating was absorbing in the visible spectrum, i.e. no light could be extracted through the coated borosilicate glass walls.

The electrical properties of the coating were measured with a multimeter and it was revealed that the coating is conductive. The resistivity value of the powder scratched from the dielectric tube was in the order of $1\text{-}2\cdot10^3$ Ohm·m, which corresponds to resistive material. However, the dielectrics used in the experiments are characterized by several orders of magnitude higher resistivity values (10^6-10^{10} Ohm·m for the borosilicate glass and 10^{10}-10^{12} Ohm·m for the alumina). It should be noted that the resistivity can change drastically with the variation of the applied frequency and temperature, thus the behavior of the material can be rather complex, considering the conditions of the DBD operation [43].

The appearance of the coating was associated with the modification of the current waveform, as shown in figure 5. The case when the conductive coating was covering both reactor walls is denoted as "Coated system" while the "Clean system" represents the condition when no conductive coating is deposited. It can be seen that the current waveform shifts from an asymmetric structure ("clean system") to a symmetric one ("coated system") with an irregular high peak structure appearing in both negative and positive HC, as described above. Interestingly, the introduction of the conductive coating and the subsequent rise of the discharge current in the negative HC had little or no influence on the efficiency of the CO_2 conversion in the MD reactor configuration. For instance, for an energy input of 60W at 0.2 SLM CO_2 flow, the conversion in the clean system was found to be 12.9%, while a value of 12 % was obtained in the coated reactor.
Another point is that the deposited structure might act as a catalyst, enhancing the backward reactions [44] and thus decreasing the effect of the current amplification.

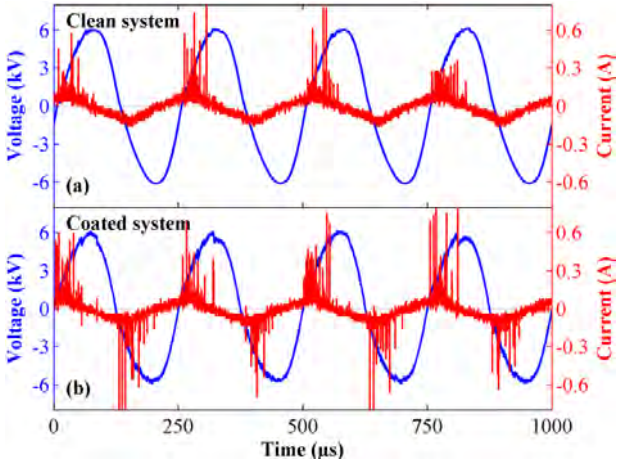

Figure 5. Electrical signal of the CO_2 DBD reactor, without the coating (a) and with the coated walls (b) (discharge power: 60W; feed flow rate: 0.6 SLM; frequency: 4 kHz; dielectric material: alumina)

The time evolution of the discharge may be presented in the following way. The charge transfer is calculated via the integration of the discharge high-current component (I>35 mA) (cf. figure 6). The modification of the current amplitude distribution for the negative HC might be spotted in this way. It is known that the charge transfer should be equal in both HCs due to the DBD capacitive nature [16,25]. However, at the beginning of the operation ("clean system") the charge balance is not observed. It can be explained by the fact that the current peaks below 35 mA are shaved out from the calculation for the case of the negative HC (figure 6, b). The coverage of the dielectric surface with a conductive coating induces the higher-current peaks, and thus the charge transferred (figure 6, "3 hours"). Ultimately, after 10 hours of operation the steady state is achieved, as the charge transfer calculated in this way is equal in both HCs. Notably, the charge transfer in the

positive HC (figure 6, a) is rather stable in time, which indicates that the coating is not influencing the discharge in the positive HC. The coverage time is highly dependent on the power input regime, ranging from tens of hours for 1-5 eV/molec. power input down to 1-3 hours for a power input of 10-15 eV/molec.

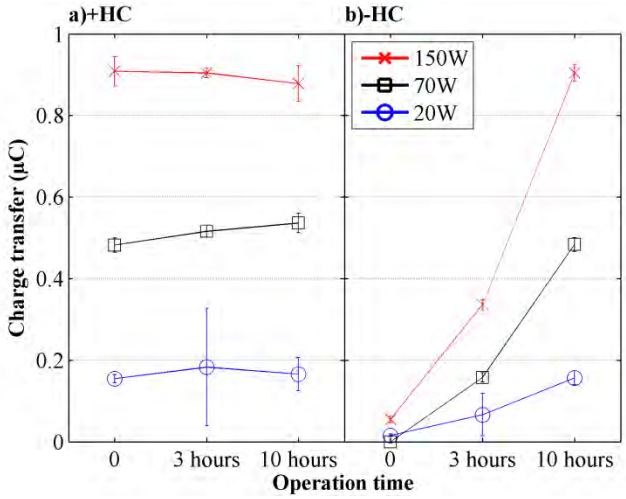

Figure 6. Charge transfer induced by the high-amplitude component of the discharge current (Idischarge>35 mA) for the cases of 150W, 70W, 20W – 4 kHz power input at 0.6 SLM CO_2.

To understand the nature of the coating, the carbon balance of the CO_2 decomposition was studied (figure 7). The carbon balance gives an indication on the percentage of the carbon fed to the reactor that is preserved in the form of CO or CO_2 after passing through the plasma reactor. Typically, the carbon balance is somewhat lower than 100%, after exposure to a plasma, meaning that some carbon is either being deposited on the reactor walls (in the form of C_2) or is transformed into higher order C species. As there is no addition of hydrogen in the system, it is safe to assume that the lowering of the carbon balance is primarily due to the surface deposition reaction. Most probably only the dissociation of CO contributes to C_2 formation, but obviously, CO itself is a product of CO_2 decomposition. Taking this into account, as well as other observations in literature on carbon deposition during CO_2 splitting [8,12], we may conclude that the carbon deposition is the result of the high peak structure in the discharge current, resulting in high conversion rates, especially at high SEI values.

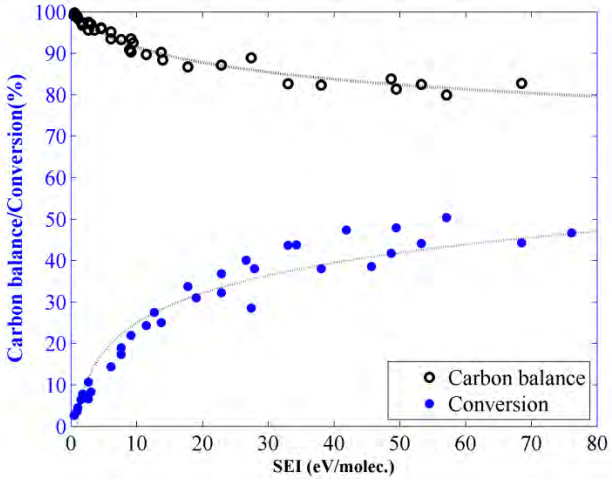

Figure 7. Carbon balance and conversion rate of CO_2 decomposition as a function of SEI. (combined data over a range of discharge frequencies and for both dielectric materials)

With respect to the modification of the current waveform, the major factor might be the appearance of a conductive surface inside the dielectric tube. Interestingly, the introduction of a

conductive coating did not influence the discharge in the positive HC, while it drastically modified the discharge in the negative HC (figure 5). In fact, a shift of the current waveform, i.e. a gradual growth of the discharge current in the negative HC, may in general be used as an indication of the appearance of a coating on the dielectric wall. If we consider the discharge configuration of the coated system in the negative HC, we can deduce that it is similar to the M-D+ configuration of the positive HC, as the cathode surface in this case is conductive as well. According to these observations, the conductivity of the cathode surface may be the crucial factor for promoting the discharge current in a CO_2 atmosphere. Unfortunately, in the case of the MD configuration, it was not possible to obtain *Q-U* Lissajous figures to evaluate the influence of the coating on the effective capacitance of the reactor.

3.3 Comparison of DD and MD configurations

3.3.1 Discharge characterisation in the various configurations

The DD configuration of the reactor was compared with the MD set-up in terms of the electrical properties of the discharge and the CO_2 conversion efficiency. Figure 8 shows the current waveforms of the CO_2 discharge in the different configurations. It can be seen that in the case of the DD configuration (figure 8, left) the discharge current is symmetric, with no high current pulses in both HCs, and thus similar to the clean M+D- system during the negative HC of the applied voltage (cf. figures 3 and 5a). To modify the existing DD configuration, a dielectric tube with a pre-deposited carbon coating on the inner surface, resulting from the previous experiments on the MD configuration, was used in the reactor (figure 6, right). As a result, the discharge current drastically rises in the negative HC and an asymmetric current waveform is observed. Again, this drastic shift in behavior was noted only in a CO_2 or O_2 atmosphere, and not in the electropositive gases (N_2, Ar, CH_4) that we studied, and to the best of our knowledge, this effect is reported for the first time. Finally, for comparison, also the current waveform of the MD configuration is again plotted (figure 8, middle) and it shows high current pulses during the positive HC (cf. figures 2, 3 and 5a above). This effect was tested over a range of the applied voltage frequencies, thus on different transformers, to validate that this phenomenon is not the result of equipment corruption. Interestingly, the formation of the coating was not observed in the DD configuration. It might reflect that the interaction with the steel electrode is crucial for the deposition process, for instance playing a role of catalyst for the disproportionation reaction (cf. equation 6).

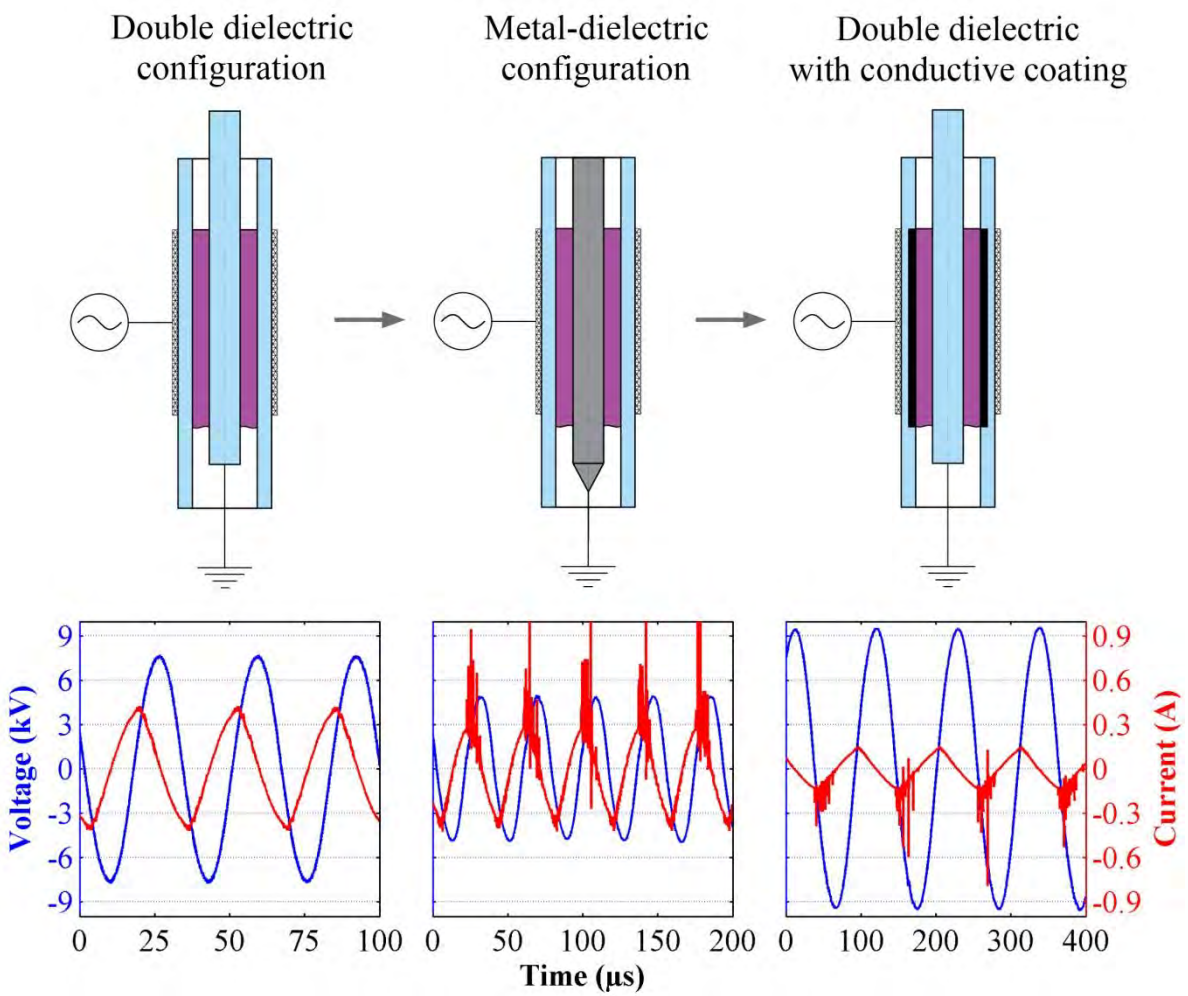

Figure 8. Comparison of the current waveforms in various reactor configurations (discharge power: 180W; CO_2 feed flow rate: 0.2 SLM; frequency (from left to right): 30 kHz; 25 kHz; 1 kHz; dielectric material: alumina).

To estimate the effect of the conductive coating on the electrical properties of the DD reactor, the relation between the transferred charge and the applied voltage was evaluated. Figure 9 depicts the Lissajous figures of this relation, averaged over 512 cycles. The figure consists of the discharge-off (DA, BC) and the discharge-on (AB, CD) lines. From the slope of these lines, we can estimate the effective capacitance (during the discharge) and the cell capacitance (when only the displacement current is present). Some changes in the Lissajous figure can be observed after the introduction of a conductive coating, indicating a variation of the sum of the cell and stray capacitances, similar to the observations by Falkenstein *et al*. [28].

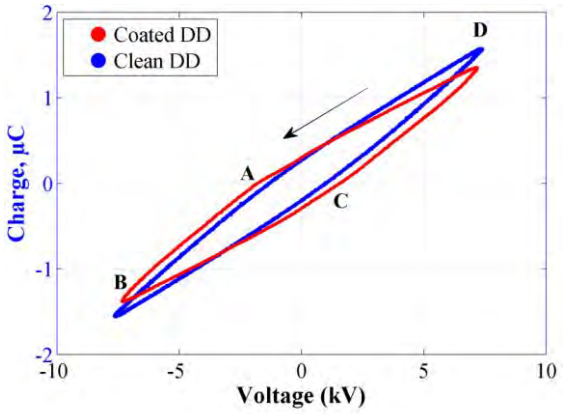

Figure 9. Lissajous figures of the CO_2 DBD in the DD configurations, with clean and coated dielectric surface (discharge power: 180W; feed flow rate: 0.2 SLM; frequency: 30 kHz; dielectric material: alumina).

By comparing the waveforms in figure 8, we can conclude that the conductivity of the cathode surface has a crucial role in the development of the CO_2 discharge current. Indeed, in the clean DD configuration, the discharge zone is composed of only non-conductive surfaces and hence the discharge current is limited in both HCs (figure 8, left). In the MD configuration (figure 8, middle), the central electrode is a metal body and consequently the high-peak discharge current structure is observed only in the positive HC, when the grounded electrode acts as a cathode. In contrast, in the DD configuration with conductive coating on the inner surface of the outer dielectric, this pre-deposited conductive film is attached to the power supply in series with the dielectric. Therefore, the coating is a cathode when the applied voltage is negative, enhancing the discharge current pulses in the negative HC (figure 8, right).

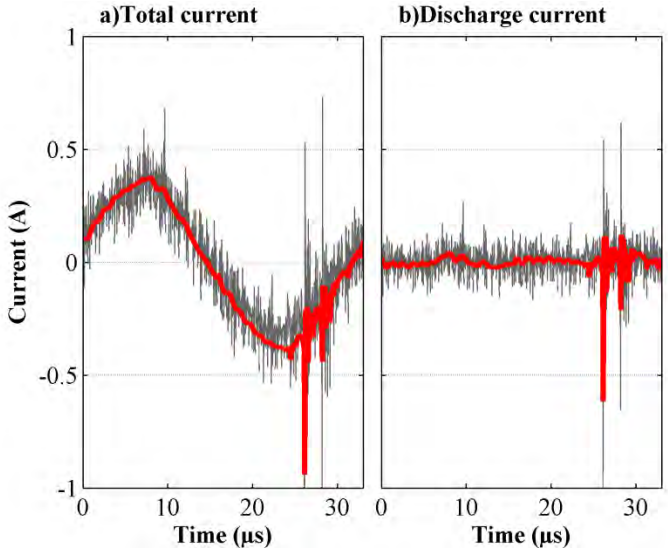

Figure 10. Comparison of current measurement by means of the Rogowski coil of the total current (a) and the discharge current (b) achieved after subtraction of the displacement current.

The validation of the Rogowski coil current measurement approach may be done by the comparison of the current signal with the derivative of the capacitor probe charge measurements (cf. figure 10) [45,46]. It can be seen that the high current peak structure is observed for the negative HC for both measurement systems, while the positive HC was free of the high-amplitude pulses. This indicates that the differences in the positive and negative HCs are related to the discharge current amplitude, and not to the detection limits of the system.

3.3.2 CO_2 conversion efficiency in the various configurations.

Figure 11 shows the CO_2 conversion rate as a function of the SEI for the MD and DD reactors, as well as for the DD configuration with a conductive coating on the inner side of the outer dielectric wall. In general, it can be stated that the conversion rises with SEI for all types of reactor configurations. The non-coated DD set-up appears to be the least efficient for the CO_2 decomposition. Upon the introduction of a conductive coating in the DD configuration (so-called coated DD), the conversion rate drastically rises, but still is somewhat lower than in the MD case. As already mentioned, a conductive coating on the inner side of the outer dielectric has limited or no impact on the conversion rate in the case of the MD configuration and thus, the data presented here cover both the "clean" and the "coated" MD configuration. The small difference in the capacitance of the clean and coated DD systems (cf. figure 9) allows a precise comparison of the process efficiency for those two reactors. However, when comparing the DD and MD configurations, some error would be inevitable due to the larger voltage drop (and thus a power loss) over the two dielectrics in case of the DD setup. This leads to an overestimation of the power input for the DD systems, when comparing to the MD one.

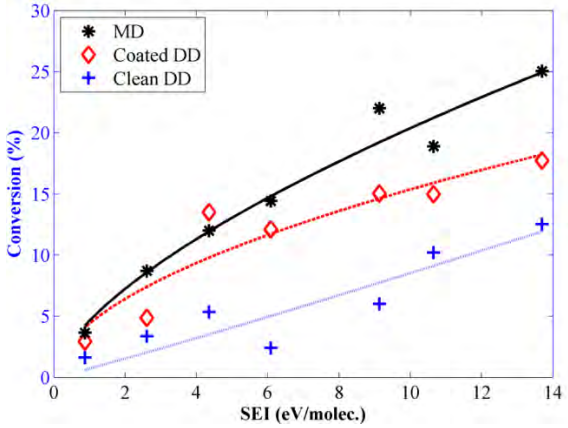

Figure 11. CO_2 conversion rate for the different DBD configurations, as a function of SEI (frequency: 10-30 kHz; dielectric material: alumina)

These results are consistent with the work of Wang *et al.* who reported that the CO_2 conversion rate was enhanced by using a custom-made high-permittivity dielectric with a controllable concentration of glass, i.e. controlled surface resistivity [9]. The differences in the conversion between the coated DD and the MD configurations may be attributed to the defects of the pre-deposited conductive coating on the dielectric surface. Indeed, visual inspection revealed uncoated areas, which might be explained by the difficulties in the coaxial geometry reactor alignment.

3.3.3 OES spectra in the various configurations

Optical emission spectroscopy is a popular technique for non-invasive *in-situ* plasma diagnostics. During the CO_2 decomposition process, the discharge was monitored with a survey spectrometer. The spectrum of the filamentary CO_2 plasma consists of CO_2/CO_2^+ lines in the range of 300-420 nm (Fox, Duffendack and Barker's System), CO 3rd positive band (280-360 nm), CO Angstroms bands in the range between 450 and 700 nm, and a continuum part with a maximum at about 450 nm [5,47-49]. No CH or C_2 Swan band lines were observed during the CO_2 experiments. In Figure 11, the optical emission spectra of the CO_2 discharge in the MD, coated DD and clean DD configurations are presented. The spectra were measured with different integration times (5000, 6000 and 8000 ms, respectively), indicating that the brightness of the discharge in the MD configuration is higher than in the coated DD configuration, and the brightness in the latter is higher than in the clean DD configuration.

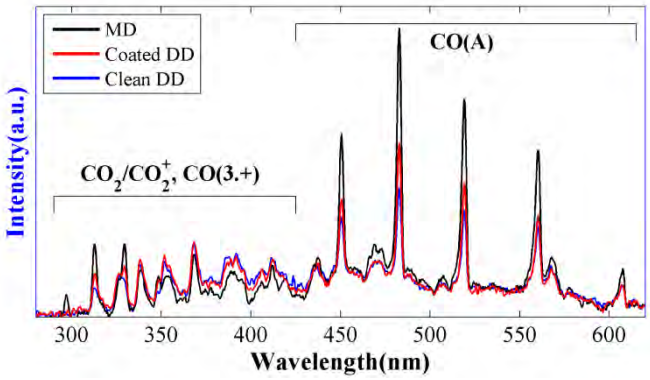

Figure 12. Emission spectra of the CO_2 DBD in MD, coated DD and clean DD configurations (discharge power: 180W; feed flow rate: 0.2 SLM; frequency: 30 kHz; dielectric material: alumina).

The emission spectra, normalized at the wavelength of 368.4 nm (as it is the most intensive peak among the CO_2/CO_2^+ lines), for the 3 configurations in the range of the brightest CO lines (450-570 nm) are shown in Figure 12.

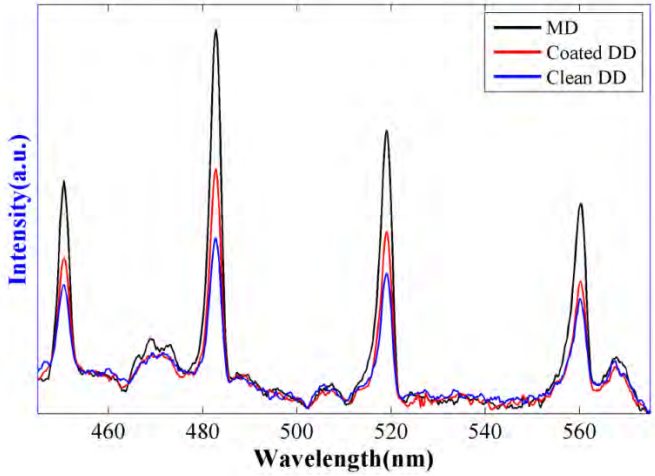

Figure 13. Emission spectra of the CO_2 DBD, in the three different configurations, normalized at 368 nm (discharge power: 180W; feed flow rate: 0.2 SLM; frequency: 30 kHz; dielectric material: alumina).

The results reveal that the luminosity of the CO_2 discharge in the clean DD configuration is much lower than in the coated DD and especially in the MD set-up. Moreover, the CO lines of the spectrum are relatively more intense in the coated DD and especially the MD reactors, while the intensity of the CO_2/CO_2^+ lines is virtually the same for all configurations (see figure 13). The fact that the CO lines are brighter for the coated DD and MD configurations might be attributed to the intense current pulses observed for these configurations. Thus, the introduction of a conductive coating in the DD configuration enhances the overall brightness of the discharge, as well as the intensity of the lines corresponding to the CO_2 decomposition process.

3.4 Discussion of the results.

In this study we observed that the CO_2 discharge significantly changes upon modification of the reactor configuration. The introduction of a conductive coating on the dielectric walls of a DBD reactor may change a range of surface properties, including the roughness, the secondary electron emission coefficient, the effective capacitance and the conductivity. Thorough screening of the various factors involved in this process reveals that the conductivity might be the most crucial parameter affecting the discharge properties [34]. The effect of the surface conductivity on the

discharge properties is somewhat contradictory in the literature, as shown in the introduction [9,33-35]. Falkenstein *et al.* reported observations similar to the ones presented here, after examining the influence of a conductive water film on a dielectric surface. In this study of a synthetic air DBD, the microdischarge intensity grew in the presence of a water film, making the bulk discharge less uniform [28]. It is interesting to note that in our reactor, the simple introduction of a conductive coating on the dielectric surface results in a notable current waveform modification, as well as in a significant improvement of the CO_2 conversion. A possible reason for this may be found in some changes in the microdischarge formation process.

Fundamental studies on the microdischarge formation report several stages of the process: pre-ionisation, cathode- and anode-oriented streamers and a decay phase [17-19,43,50]. It is known that charge transfer (i.e. a current pulse) starts after the cathode-oriented streamer reaches the surface of the electrode [17]. At this point, electrons are directed towards the anode through a conductive channel, left after the previous phase. In the case of the M-D+ configuration, electrons are supplied from the metal surface. The surface discharge preceding the current transfer is responsible for this process in case of the dielectric cathode, creating a conductive sheet on top of the barrier [28]. Akishev *et al.* introduced the term "local barrier capacitance" for this phenomenon that limits the current passing through the single microdischarge [41,42]. In this work, the dielectric was presented in the form of multiple parallel capacitances, connected by a series of resistances on the surface. The local barrier capacitance may be increased by decreasing the surface resistance in this way, i.e. more electrons might be supplied to the microdischarge channel, forming the current pulse. It seems to be a possible explanation for the discharge current rise when a conductive coating is acting as the cathode surface (figures 4, 6). Notably, the conductive surface acting as the anode does not influence the discharge (cf. asymmetric waveform of the clean MD system in figure 4,a and the coated DD configuration in figure 6).

Again, the current waveforms are a superposition of multiple microdicharges over time, thus we cannot spot differences of single microdischarge behaviour in this setup. For this aim, single filament DBD reactors were utilised [19], producing fundamental data on these processes. Nevertheless, we tried to correlate various analysis methods with the bulk discharge current oscillograms. For the clean DD set-up, the discharge current was limited and resembled that of the M+D- configuration. The CO_2 conversion rate and the discharge brightness were correspondingly limited in this case. The introduction of a conductive coating on the dielectric wall enhanced the discharge current peaks in the HC corresponding to the time when this surface was acting as a cathode. Consequently, the conversion efficiency and the emission of the CO lines were amplified. In the case of the MD configuration, the conversion rate was the highest and a conductive carbon coating was deposited on the reactor walls. We can therefore assume that microdischarges of higher intensity occur in case of high-peak discharge current structure, leading to the formation of more CO (due to CO_2 decomposition) and possibly to the formation of a carbon coating on the reactor walls. The fact that the conversion rate did not rise upon coating appearance in the MD configuration might be explained by the CO disproportionation reaction (6) [51]:

$$2\,CO \rightarrow C + CO_2 \qquad (6)$$

This reaction might limit the conversion efficiency and lead to the formation of the carbon coating on the reactor walls.

According to the current waveforms, the CO_2 discharge is composed of numerous low-amplitude filaments in the clean DD configuration. For the case of the coated DD or MD configurations, sparse high-amplitude current pulses are observed, which could be related to stronger and rare filaments, appearing in the channels of previously extinguished filaments [40]. It might be deduced that different plasma parameters correspond to streamers of those two regimes, as n_e, T_e, should be higher for high-current regimes. From the presented results it might be concluded that high-current pulses, although rather sparse and non-uniformly distributed, are more favourable for CO_2 conversion.The deposited conductive coating is shown to amplify the discharge current, however probably enhancing the backward reaction at the same time. This indicates that a more precise choice of a conductive catalytic coating on the dielectric wall may be beneficial for the process efficiency.

The phenomena of the conductivity influence on the discharge current may be further studied in a parallel-plate reactor. A controlled conductivity of the dielectric surface may be achieved by thin film deposition techniques. For instance, a thin layer of chromium would possibly allow the utilization of an optically transparent DBD system, resistant to the oxidation of the CO_2 discharge. In this way the measurements of the discharge current might be correlated with the conductivity of the surface, speed imaging of the filaments and conversion efficiency. Additionally, the analysis of the solid products of the CO_2 discharge would be more straightforward in this case.

In summary, it was shown that the microdischarge activity of a DD type DBD reactor and the process efficiency in CO_2 splitting can be significantly modified by the introduction of a conductive film on the dielectric surface. In this way, the appearance of a conductive coating can be considered as an activation step for the DD configuration. Indeed, typically high-permittivity dielectric materials are utilized when higher conversion rates and high-peak discharge currents are observed [7-9]. In our work, similar effects were observed upon the introduction of a conductive coating on the surface of conventional dielectric materials (borosilicate glass and alumina). This property might be applied in fundamental studies of DBD systems, where DD reactors are commonly used [4,5], to simulate processes in the MD configuration.

However, the MD configuration of the DBD reactor seems to be more advantageous for the CO_2 decomposition technology, as the highest rates of CO_2 conversion efficiency were achieved in this configuration. Besides, the MD configuration presents a better solution in terms of design based on robust constructional materials.

4. Conclusion

In this work it was shown that the surface conductivity has a prominent role in the CO_2 discharge in a DBD reactor with various configurations:

(i) In the clean MD configuration, the CO_2 discharge current was asymmetric, with a high-peak discharge current structure observed during the positive HC (denoted as M-D+);

(ii) During the CO_2 decomposition process, a conductive coating was found to be covering the reactor walls, and subsequently changing the current waveform into a symmetric waveform with current peaks in both the positive and negative HC;

(iii) In the clean DD configuration, the discharge current was limited in both HCs, similar to the M+D- phase of the clean MD reactor;

(iv) In the DD configuration, when using the dielectric tube with pre-deposited conductive coating, i.e., so-called coated DD configuration, the CO_2 conversion efficiency, the optical emission signal, and the discharge current in the negative HC were significantly higher than in the clean DD configuration.

All this indicates that the microdischarge activity drastically changes when the conductive surface acts as a cathode. In this way it is possible to control the CO_2 conversion efficiency and modify the microdischarge formation process in the DD reactor without using elaborated dielectric materials.

5. Acknowledgment

The research leading to these results has received funding from the European Union Seventh Framework Programme (FP7-PEOPLE-2013-ITN) under Grant Agreement № 606889 (RAPID - Reactive Atmospheric Plasma processIng – eDucation network).

Reference

[1] Fridman A 2008 *Plasma Chemistry* (Cambridge University Press: New York)

[2] Paullusen S, Verheyde B et al. 2010 Conversion of carbon dioxide to value-added chemicals in atmospheric pressure dielectric barrier discharges *Plasma Sources Science and Technology* **19** 034015

[3] Wang J Y, Xia G G et al. 1999 CO_2 Decomposition Using Glow Discharge Plasmas *Journal of Catalysis* **185** 152-9

[4] Brehmer F, Welzel S et al. 2015 CO and byproduct formation during CO_2 reduction in dielectric barrier discharges *Journal of Applied Physics* **116**

[5] Brehmer F 2015 Shining light on transient CO_2 plasma *PhD Thesis* Technical University of Eindhoven

[6] Aerts R, Somers W et al. 2015 Carbon Dioxide Splitting in a Dielectric Barrier Discharge Plasma: A Combined Experimental and Computational Study *ChemSusChem* **8** 702-16

[7] Li R, Tang Q et al. 2006 Plasma catalysis for CO_2 decomposition by using different dielectric materials *Fuel Processing Technology* **87** 617-22

[8] Li R, Tang Q et al. 2007 Investigation of dielectric barrier discharge dependence on permittivity of barrier materials *Applied Physics Letters* **90** 131502

[9] Wang S, Zhang Y et al. 2012 Enhancement of CO_2 Conversion Rate and Conversion Efficiency by Homogeneous Discharges *Plasma Chem Plasma Process* **32** 979-89

[10] Mei D, Zhu X et al. 2015 Plasma-assisted conversion of CO_2 in a dielectric barrier discharge reactor: understanding the effect of packing materials *Plasma Sources Science and Technology* **24** 015011

[11] Van Laer K and Boagaerts A 2015 Improving the converson and energy efficiency of CO_2 splitting in a ZrO_2 packed bed DBD reactor *Energy Technol.(in press)*

[12] Zheng G, Jiang J et al. 2003 The Mutual Conversion of CO_2 and CO in Dielectric Barrier Discharge (DBD) *Plasma Chemistry and Plasma Processing* **23** 59-68

[13] Lindon M A and Scime E 2014 CO_2 Dissociation using the Versatile Atmospheric Dielectric Barrier Discharge Experiment (VADER) *Frontiers in Physics* **2**

[14] Ramakers M, Michielsen I et al. 2015 Effect of argon or helium on the CO_2 conversion in a dielectric barrier discharge *Plasma Process.Polym.* **12** 755-63

[15] Petrovic D 2009 Fluid modelling of an atmospheric pressure dielectric barrier discharge in cylindrical geometry *Journal of Physics D: Applied Physics* **42** 205206

[16] Stollenwerk L and Stroth U 2011 Electric Charging in Dielectric Barrier Discharges with Asymmetric Gamma-Coefficients *Contrib.Plasma Phys.* **51** 61-7

[17] Gibalov V I and Gerhard J P 2000 The development of dielectric barrier discharges in gas gaps and on surfaces *Journal of Physics D: Applied Physics* **33** 2618

[18] Gibalov V I and Gerhard J P 2012 Dynamics of dielectric barrier discharges in different arrangements *Plasma Sources Science and Technology* **21** 024010

[19] Hoder T, Brandenburg R et al. 2010 A comparative study of three different types of barrier discharges in air at atmospheric pressure by cross-correlation spectroscopy *Journal of Physics D: Applied Physics* **43** 124009

[20] Enloe C L, McLaughlin T E et al. 2004 Mechanisms and Responses of a Single Dielectric Barrier Plasma Actuator: Plasma Morphology *AIAA Journal* **42** 589-94

[21] Enloe C L, McHarg M et al. 2009 Plasma-induced Force and Self-induced Drag in the Dielectric Barrier Discharge Aerodynamic Plasma Actuator *47th AIAA Aerospace Sciences Meeting including The New Horizons Forum and Aerospace Exposition*

[22] Šimek M, Pekárek S et al. 2010 Influence of Power Modulation on Ozone Production Using an AC Surface Dielectric Barrier Discharge in Oxygen *Plasma Chem Plasma Process* **30** 607-17

[23] Šimek M, Pekárek S et al. 2012 Ozone Production Using a Power Modulated Surface Dielectric Barrier Discharge in Dry Synthetic Air *Plasma Chem Plasma Process* **32** 743-54

[24] Pekárek S 2013 Asymmetric properties and ozone production of surface dielectric barrier discharge with different electrode configurations *Eur.Phys.J.D* **67** 1-7

[25] Allegraud K, Guaitella O et al. 2007 Spatio-temporal breakdown in surface DBDs: evidence of collective effect *Journal of Physics D: Applied Physics* **40** 7698
[26] Biganzoli I, Barni R et al. 2013 Optical and electrical characterization of a surface dielectric barrier discharge plasma actuator *Plasma Sources Science and Technology* **22** 025009
[27] Benard N and Moreau E 2014 Electrical and mechanical characteristics of surface AC dielectric barrier discharge plasma actuators applied to airflow control *Exp Fluids* **55** 1-43
[28] Falkenstein Z and Cogan J 1997 Microdischarge behaviour in the silent discharge of nitrogen - oxygen and water - air mixtures *Journal of Physics D: Applied Physics* **30** 817

[30] Futamura S and Kabashima H 2004 Synthesis Gas Production from CO_2 and H_2O with Nonthermal Plasma **153** 119-24
[31] Tomai T, Ito T et al. 2006 Generation of dielectric barrier discharge in high-pressure N_2 and CO_2 environments up to supercritical conditions *Thin Solid Films* **506–507** 409-13
[32] Tomai T, Katahira K et al. 2007 Carbon materials syntheses using dielectric barrier discharge microplasma in supercritical carbon dioxide environments *The Journal of Supercritical Fluids* **41** 404-11
[33] Kim Y, Cha M S et al. Characteristics of Dielectric Barrier Glow Discharges with a Low-Frequency Generator in Nitrogen *Journal of Korean Physical Society* **43**
[34] Choi S, Joo H N et al. 2006 Improvement of plasma uniformity using ZnO-coated dielectric barrier discharge in open air *Plasma Science, ICOPS 2006 The 33rd IEEE Int.Conf.* p61
[35] Guoqing Y, Anbang L et al. 2013 Effect of Dielectric Surface Conductivity on Atmospheric Dielectric Barrier Discharge *Electrical Insulation and Dielectric Phenomena (CEIDP), 2013 IEEE Conf.* pp278-82
[36] Xin T, Hellen J G et al. 2011 Dry reforming of methane over a Ni/Al_2O_3 catalyst in a coaxial dielectric barrier discharge reactor *Journal of Physics D: Applied Physics* **44** 274007
[37] Snoeckx R, Zeng Y X et al. 2015 Plasma-based dry reforming: improving the conversion and energy efficiency in a dielectric barrier discharge *RSC Adv.* **5** 29799-808
[38] Guaitella O, Thevenet F et al. 2006 Dynamic of the plasma current amplitude in a barrier discharge: influence of photocatalytic material *Journal of Physics D: Applied Physics* **39** 2964
[39] Kozlov K V, Brandenburg R et al. 2005 Investigation of the filamentary and diffuse mode of barrier discharges in N_2/O_2 mixtures at atmospheric pressure by cross-correlation spectroscopy *Journal of Physics D: Applied Physics* **38** 518
[40] Audier P, Rabat H et al. 2014 Experimental investigation of a surface DBD actuator at atmospheric pressure in different N_2/O_2 gas mixtures *Plasma Sources Science and Technology* **23** 065045
[41] Akishev Y, Aponin G et al. 2011 'Memory' and sustention of microdischarges in a steady-state DBD: volume plasma or surface charge? *Plasma Sources Science and Technology* **20** 024005
[42] Akishev Y S, Aponin G et al. 2011 Role of the volume and surface breakdown in a formation of microdischarges in a steady-state DBD *Eur.Phys.J.D* **61** 421-9
[43] Samoilovich V G, Gibalov V I and Kozlov K V 1997 *Physical Chemistry of the Barrier Discharge* (Deutscher Verlag für Schweisstechnik) p261
[44] Spencer L F and Gallimore A D 2013 CO_2 dissociation in an atmospheric pressure plasma/catalyst system: a study of efficiency *Plasma Sources Science and Technology* **22** 015019
[45] Pai D, Strauss S et al. 2014 Surface dielectric barrier discharges exhibiting field emission at high pressures *Plasma Sources Science and Technology* **23** 025019
[46] Pai D, Strauss S et al. 2015 Field-emitting Townsend regime of surface dielectric barrier discharges emerging at high pressure up to supercritical conditions *Plasma Sources Science and Technology* **24** 025021
[47] Fox G W, Duffendack O S et al. 1927 The Spectrum of CO_2 *Proc.Natl.Acad.Sci.USA* **13(5)** 302-7

[48] Silva T, Britun N et al. 2014 Optical characterization of a microwave pulsed discharge used for dissociation of CO_2 *Plasma Sources Science and Technology* **23** 025009
[49] Oh T 2013 Dissociation of Carbon Dioxide in Atmospheric Pressure Microchannel Plasma Devices *MSc Thesis* University of Illinois at Urbana-Champaign
[50] Brandenburg R, Bogaczyk M et al. 2013 Novel insights into the development of barrier discharges by advanced volume and surface diagnostics *Journal of Physics D: Applied Physics* **46** 464015
[51] Li M, Xu G et al. 2004 Carbon Dioxide Reforming of Methane Using DC Corona Discharge Plasma Reaction *J.Phys.Chem.A* **108** 1687-93